S100 calcium-binding protein A16 suppresses the osteogenic differentiation of rat bone marrow mesenchymal stem cells by inhibiting SMAD family member 4 signaling

JING XIN, ZHAOXU WANG, YANJU SHEN, JING BAI and YAFEI SHEN

Department of Endocrinology and Diabetes, Luohe Central Hospital, Luohe First People's Hospital,
The First Affiliated Hospital of Luohe Medical College, Luohe, Henan 462000, P.R. China

Abstract. Osteogenesis is a complex process of bone formation regulated by various factors, yet its underlying molecular mechanisms remain incompletely understood. The present study aimed to investigate the role of S100A16, a novel member of the S100 protein family, in the osteogenic differentiation of rat bone marrow mesenchymal stem cells (BMSCs) and uncover a novel Smad4-mitogen-activated protein kinase (MAPK)/Jun N-terminal kinase (JNK) signaling axis. In the present study, the expression level of S100A16 in bone tissues and BMSCs from ovariectomized rats was evaluated and then the impact of S100A16 silencing on osteogenic differentiation was examined. Increased S100A16 expression was observed in bone tissues and BMSCs from ovariectomized rats, and S100A16 silencing promoted osteogenic differentiation. Further transcriptomic sequencing revealed that the Smad4 pathway was involved in S100A16 silencing-induced osteogenesis. The results of western blot analysis revealed that S100A16 overexpression not only downregulated Smad4 but also activated MAPK/JNK signaling, which was validated by treatment with MAPK and JNK inhibitors U0126 and SP600125. Overall, in the present study, the novel regulatory factors influencing osteogenic differentiation were elucidated and mechanistic insights that could aid in the development of targeted therapeutic strategies for patients with osteoporosis were provided.

Correspondence to: Dr Yafei Shen, Department of Endocrinology and Diabetes, Luohe Central Hospital, Luohe First People's Hospital, The First Affiliated Hospital of Luohe Medical College, 56 Renmin East Road, Zhaoling, Luohe, Henan 462000, P.R. China
E-mail: doctorlove2011@163.com

Introduction

Osteogenesis is the continuous process of bone formation that occurs throughout an individual's life. This complex process relies on the coordination between osteoblasts, which are specialized cells responsible for synthesizing bone tissue, and osteoclasts, which are involved in the breakdown and remodeling of existing bone (1,2). Osteogenic differentiation is a specific cellular process involving the transformation of certain stem cells or precursor cells into osteoblasts. This complex process encompasses a series of cellular and molecular events. Signaling pathways, including the Wnt/β-catenin (3,4) and bone morphogenetic protein pathways (5,6), play significant roles in promoting osteoblast differentiation by activating specific genes. Transcription factors also contribute to stem cell differentiation toward an osteogenic lineage. Runx2, known as a master regulator of osteogenesis, controls the expression of genes critical for osteoblast maturation and bone mineralization (7,8). Other transcription factors, such as Osterix and Dlx5, are involved in regulating osteogenic differentiation (9,10).

Among the mentioned factors affecting osteogenic differentiation, S100 calcium-binding protein A16 (S100A16), a novel member of the S100 protein family, had been reported to be involved in this process based on a mouse model (11). S100A16, which is expressed widely, including in adipose tissues, has been associated with various human diseases, including inflammation disorders, prostate cancer and obesity (12). As a calcium-binding protein, S100A16 binds one calcium ion per monomer. *In vitro* studies suggest that it can promote adipocyte differentiation. S100A16 overexpression in preadipocytes induces increased proliferation, enhances adipogenesis, and reduces insulin-stimulated glucose uptake (11). Gene Ontology (GO) annotations revealed its involvement in protein homodimerization activity. Previous studies in mouse models have demonstrated that S100A16 inhibits osteogenesis but stimulates adipogenesis (11). However, the role of S100A16 in the osteogenic differentiation of bone marrow mesenchymal stem cells (BMSCs) from rats and underlying mechanisms remain unexplored.

Additionally, extracellular matrix proteins, including collagen and various growth factors, such as transforming

growth factor-beta (TGF-β), play vital roles in promoting osteogenic differentiation (13,14). These factors provide the necessary microenvironment and signaling cues for stem cells to undergo osteogenic lineage commitment and subsequent bone formation. As a part of the TGF-β signaling pathway, the Smad4 gene encodes a protein involved in transmitting chemical signals from the cell surface to the nucleus, allowing external factors to influence gene activity and protein production within the cells (15). Furthermore, Smad4 serves as both a transcription factor and a tumor suppressor. However, the specific function of Smad4 in osteogenic differentiation has not yet been studied.

The mitogen-activated protein kinase (MAPK)/c-Jun N-terminal kinase (JNK) pathway is another important pathway implicated in osteogenesis. Smad4 has been reported to have an impact on this pathway. In fact, in a previous study in human pancreatic carcinoma it was found that Smad4 downregulated JNK activity and while also inhibiting thyroid cancer cell growth by inactivating the MAPK/JNK pathway (16). However, the role of the MAPK/JNK pathway in osteogenesis remains controversial. A certain study suggested that bone morphogenetic protein-9 enhances the osteogenic differentiation of human periodontal ligament stem cells via the JNK pathway (17), whereas another found that the MAPK/JNK signaling pathway suppresses the osteogenic differentiation of MC3T3-E1 osteoblasts under titanium ion exposure conditions (18).

The current study examined the role of S100A16 and Smad4 in the osteogenic differentiation of rat BMSCs and investigated the impact of the novel S100A16-Smad4-MAPK/JNK signaling axis in this process. Furthermore, MAPK/JNK inhibitors and small interfering (si)RNAs that repressed the expression of S100A16 were further applied to determine their effects on the osteogenic differentiation of rats BMSCs, as well as the expression of key genes. Additionally, ovariectomized (OVX) rats serve as a prevalent animal model in osteoporosis research within the medical field. Rats achieve sexual and endocrine system maturation at 3 months, coinciding with well-formed muscles and skeleton (19). Furthermore, ovariectomy in rats, which involves the removal of ovaries and subsequent estrogen deficiency, has been associated with increased differentiation of BMSCs toward osteogenic pathways (20). Estrogen is a key regulator of bone homeostasis that inhibits bone resorption and promotes bone formation. In the absence of estrogen, as observed in OVX rats, BMSCs are stimulated to undergo osteogenic differentiation. This response is part of an adaptive mechanism that counteracts the increased bone resorption, contributing to the accelerated bone turnover observed in this experimental model. Therefore, OVX female Sprague-Dawley rats were used in the present study to investigate the osteogenesis *in vivo*. Overall, novel regulation factors that affect osteogenic differentiation were discovered and new mechanistic evidence for developing targeted and effective therapeutic strategies for patients with osteoporosis was ultimately provided.

Materials and methods

Animals and ovariectomy. A total of 30 8-week-old (180-200 g) female Sprague-Dawley rats were purchased from Charles River Beijing Co., Ltd. All rats were housed in a specific pathogen-free facility under a 12-h light/12-h dark cycle, with a controlled room temperature of 25°C, and provided *ad libitum* access to food and water. Ovariectomy was performed as previously described (21). Briefly, rats were injected intraperitoneally with pentobarbital (30 mg/kg), followed by exposure and excision of the ovaries from both sides. Rats in the sham group underwent similar procedures except that their ovaries were left intact. Following surgery, all animals, including the sham rats, were sutured and received penicillin injections for three consecutive days. Sprague-Dawley rats were used for bone marrow stem cell isolation and establishing the OVX rat model. It was confirmed that all animals were treated following the IACUC guidelines. The present study was approved (approval no. 2020018) by the animal Ethics Committee of Luohe Central Hospital (Luohe, China).

Isolation of BMSCs and cell culture. All rats were sacrificed via cervical dislocation and then the whole rats were immersed in 75% ethanol for 15 min for sterilization. Bone marrow cells were isolated from Collum femoris with DMEM (Shanghai BasalMedia Technologies Co., Ltd.) and cultured at a temperature of 37°C in the presence of 5% CO_2. After three passages, BMSCs were characterized by hematopoietic markers (CD11b and CD45) and BMSC markers (CD90 and CD44) using a CytoFLEX nano flow cytometer (Beckman Coulter, Inc.). The flow cytometry data were analyzed by Kaluza Analysis Software (version 2.1.1; Beckman Coulter, Inc.). The antibodies used were as follows: PE-conjugated mouse anti-CD11b antibody (cat. no. sc-53086; Santa Cruz Biotechnology, Inc.), PE-conjugated mouse anti-CD45 antibody (cat. no. 202207; BioLegend, Inc.), PE-conjugated mouse anti-CD90 antibody (cat. no. 202523; BioLegend, Inc.), and PE-conjugated mouse anti-CD44 antibody (cat. no. sc-7297; Santa Cruz Biotechnology, Inc.). All *in vitro* experiments were performed using cells from passages 3-5.

Differentiation of BMSCs. BMSCs ($2.0x10^4$) were seeded into HyCyte™ rat BMSC culture medium (Cas9X Biotech Co. Ltd.) and were allowed to attach for 24 h, after which the medium was replaced with HyCyte™ osteogenic differentiation medium (Cas9X) and changed every 3 days. After 14 days, cells were fixed with 4% polyformaldehyde for 15 min and then stained with 0.1% sodium alizarin sulfonate-Tris-HCL staining solution (pH=8.3) for 30 min at 37°C. Stained cells were then washed with PBS and imaged through a light microscopy. For inhibitor treatments, both U0126 (cat. no. T21332; TargetMol Chemicals Inc.) and SP600125 (cat. no. T3109; TargetMol Chemicals Inc.) were used at a concentration of 10 μM.

siRNA interference assay. S100A16 and negative control siRNA were purchased from Shanghai GenePharma Co., Ltd. with their sequences being as follows: si-S100A16-1 forward, 5'-GAAUUAGCCUCUUCUCUUC-3' and reverse, 5'-GAAGAGAAGAGGCUAAUUC-3'; si-S100A16-2 forward, 5'-UAUGUAUCCAAGCACAGCC-3' and reverse, 5'-GGCUGUGCUUGGAUACAUA-3'; si-S100A16-3 forward, 5'- AGAACAAGAUCAGCAAGUC-3' and reverse, 5'-GACUUGCUGAUCUUGUUCU-3'; scrambled negative control forward, 5'-UUCUCCGAACGUGUCACGU-3'

and reverse, 5'-ACGUGACACGUUCGGAGAA-3'. BMSCs were transfected with 50 nM of desired the siRNAs using Lipofectamine 3000 in Opti-MEM® at 37˚C (Thermo Fisher Scientific Inc.) on days 0, 3, 5, 7, 9 and 12 of differentiation. At 6 h after transfection, the medium was replaced with osteogenic differentiation medium and changed every 3 days. The total RNA of each sample was isolated and sequenced on day 14 of differentiation.

Hematoxylin and eosin (H&E) staining. Rat femurs were dissected, fixed in 4% formaldehyde at room temperature for 2 days, and subsequently decalcified in EDTA solution at room temperature over a period of 4 weeks. Following decalcification, the specimens underwent dehydration and were processed to form paraffin blocks. Serial transverse and longitudinal sections, each 5-μm thick, were then prepared from both the diaphysis and metaphysis of the femurs. These sections were subjected to H&E and Masson's trichrome staining. All sections were examined using a light microscope, allowing for a comprehensive analysis of the bone tissue structure and composition.

Alizarin red S staining. Cells were initially washed three times with PBS before fixation in absolute ethanol for 30 min, followed by complete air drying. Subsequently, Alizarin Red S Solution (0.2%; pH8.3; Beijing Solarbio Science & Technology Co., Ltd.) was added to the plates, after which the cells were incubated at room temperature for 15 min. After incubation, the cells were carefully rinsed with double-distilled water and allowed to air dry. Stained cells were examined using light microscopy and photographed.

Western blot analysis. For bone tissue protein extraction, a bone tissue protein extraction kit (Beijing Solarbio Science & Technology Co., Ltd.) was used. RIPA buffer (Beyotime Institute of Biotechnology) was used for cellular protein extraction. The protein content in all lysates was measured using a BCA protein quantification kit (Beyotime Institute of Biotechnology) and 10 μg of protein from each sample was loaded and allowed to run on a 10% sodium dodecyl-sulfate polyacrylamide gel, connected to an electric source. The overall protein on the gel was then transferred to a polyvinylidene difluoride membrane, which was then blocked using 1% BSA (Beyotime Institute of Biotechnology) for 1 h at room temperature. Thereafter, the sample was incubated overnight at 4˚C with primary antibodies that detect and bind to the specific protein of interest. The membrane was then washed with Tris-buffered saline with 0.02% Tween 20 (TBST) and then incubated with horseradish peroxidase (HRP)-linked secondary antibody for 1 h. Afterwards, the membrane was once again washed with TBST. The chemiluminescent HRP-substrate was then added to the blot, and a Tanon 5200 automatic chemiluminescence image analysis system (Shanghai Tianneng Life Science Co., Ltd.) was used to detect the protein of interest. ImageJ software (v1.50b; National Institutes of Health) was used for the quantification of the protein bands. The antibodies used in the present study were as follows: rabbit anti-S100A16 antibody (1:1,000; cat. no. A16167), rabbit anti-GAPDH antibody (1:5,000; cat. no. AC001), rabbit anti-RUNX2 antibody (1:500; cat. no. A11753,), rabbit anti-SMAD4 antibody (1:1,000; cat. no. A21487), rabbit anti-MAPK antibody (1:1,000; cat. no. A14401), rabbit anti-phospho-MAPK antibody (1:2,000; cat. no. AP0526), rabbit anti-JNK1 antibody (1:1,000; cat. no. A2462), rabbit anti-OSTERIX antibody (1:1,000;

cat. no. A18699; all from ABclonal Biotech Co., Ltd.), rabbit anti-JNK antibody (1:1,000; cat. no. 80024-1-RR; Proteintech Group, Inc.) and HRP-conjugated goat anti-rabbit secondary antibody (1:10,000; cat. no. AS014; ABclonal Biotech Co., Ltd.).

Reverse transcription-quantitative PCR (RT-qPCR). The total RNA of each cell lysate sample was extracted using a SteadyPure RNA extraction kit (Accurate Biology Co., Ltd.) following the manufacturer's protocol. For bone tissue RNA extraction, a SPARKeasy bone tissue RNA extraction kit (Sparkjade biotech Co. Ltd.) was used. The HiFiScript cDNA Synthesis Kit (CWBio) was used to reverse transcribe cDNA from the isolated RNAs according to the manufacturer's instructions. The expression of the genes of interest was determined using qPCR with SYBR Green Pro Taq HS master mix (Hunan Aikerui Bioengineering Co., Ltd.). The thermocycling conditions consisted of an initial denaturation step at 95˚C for 1 min, followed by denaturation at 95˚C for 10 sec, and annealing and extension at 60˚C for 20 sec. This cycle was repeated 40 times. The relative expression was calculated using the $2^{-\Delta\Delta Cq}$ method as reported previously (22). The sequences of primers used for the genes of interest are listed in Table I. The relative mRNA expression of the desired genes was determined using human GAPDH as internal control.

RNA sequencing and bioinformatics analysis. The total RNA of each cell lysate sample was extracted from siRNA interference or scramble groups using RNeasy Mini Kit (cat. no. 74104; Qiagen China Co., Ltd.) following the manufacturer's instruction. Thereafter, RNA sequencing (RNAseq) was performed on 2 μg RNA from each sample using Illumina HiSeq™. Sequencing libraries of nucleotides with length of 300-600 bp (5'-3') were generated using Unicellular RNAseq Library Prep Kit (cat. no. AT4205-01; Hangzhou Kaitai Biotech Co., Ltd.). HISAT2 software (version 2.1.0; http://daehwankimlab. github.io/hisat2/) and DESeq2 software (version 1.14.1; https://bioconductor.org/packages/release/bioc/html/DESeq2. html) were used to identify differentially expressed genes (DEGs) between each sample using the following filter criteria: P<0.05 and the absolute value of log$_2$FC >1. DEGs were annotated using the DAVID database (https://david.ncifcrf.gov/) to examine the enriched GO terms. Gene set enrichment analysis (GSEA) was performed using GSEA software (Version 4.3.2; https://www.gsea-msigdb.org/gsea/index.jsp?).

Statistical analysis. Significance differences between the groups were determined using unpaired Student's t-test or one-way ANOVA followed by Dunnett's test using GraphPad Prism software (version 9.5.1.733; Dotmatics). Each experiment was performed with at least three biological repeats and the results were presented as the mean with standard errors. P<0.05 was considered to indicate a statistically significant significance.

Results

S100A16 levels in OVX rats and BMSCs. The OVX rat model was established through bilateral ovariectomy and utilized to mimic estrogen deficiency-induced bone loss. H&E and Masson's staining of bone tissues from wild-type (WT) rats confirmed the occurrence of osteoporosis. Specifically, H&E

Table I. Primers used in reverse transcription-quantitative PCR used in the present study.

Gene name	Primer sequence (5'-3')
S100A16	F: GAGCTGAGGCAGTGAGATGG
	R: ACCAGGCTGTGCTTGGATAC
RUNX2	F: AGTCTGTCTGGCGACCCTAT
	R: TTGCCAGATCACAACTGGGG
OSX	F: ACCTCTTGAGAGGAGACGGG
	R: CTGTTGAGTCTCGCAGAGGG
OCN	F: GAGGACCCTCTCTCTGCTCA
	R: GGTAGCGCCGGAGTCTATTC
ALP	F: GGCACCATGACTTCCCAGAA
	R: ACCGTCCACCACCTTGTAAC
SMAD4	F: GCTGGGAACTCAGCCCTCTA
	R: GCAGCTCGTTCAGCAATGAC
GAPDH	F: TGGTGAAGGTCGGTGTGAAC
	R: GATGGTGATGGGTTTCCCGT

F, forward; R, reverse; Runx2, RUNX family transcription factor 2; OSX, osterix; OCN, osteocalcin; ALP, alkaline phosphatase.

staining showed the replacement of trabeculae by adipocytes in the bone marrow of the femoral shaft of OVX rats (Fig. 1A), whereas Masson's staining indicated reduced collagen fiber content and decreased levels of new bone in OVX rats (Fig. 1B). A comparison of S100A16 expression at the mRNA and protein levels in bone tissues isolated from OVX and sham-operated rats demonstrated significantly enhanced expression in the OVX group (Fig. 1C and D). Next, BMSCs were isolated from rat bone tissues, after which specific markers were characterized using flow cytometry. As demonstrated in Fig. 1E, BMSCs were positive for traditional BMSC markers (CD90 and CD44) but were negative for hematopoietic markers (CD34 and CD45), confirming the successful isolation of BMSCs suitable for downstream experiment. In addition, S100A16 mRNA expression levels were significantly higher in BMSCs from OVX rats than in those from the sham group (Fig. 1F). Collectively, both the *in vivo* rat model and *in vitro* BMSC model demonstrated enhanced S100A16 levels in the OVX groups, suggesting a potential pivotal role for this gene in osteoporosis.

Role of S100A16 in osteogenic differentiation of rat BMSCs. To investigate the role of S100A16 in osteoporosis, siRNAs were further utilized to knockdown S100A16 in BMSCs and determine its effects on osteogenic differentiation. First, three siRNAs targeting S100A16 were tested in terms of their efficiency in knocking down BMSCs isolated from WT rats. As revealed in Fig. 2A, siRNAs 1 and 3 exhibited a knockdown efficiency of over 60% compared with the scramble control, with siRNA 3 producing the highest efficiency, leading to its use in subsequent downstream experiments. Next, Alizarin Red S staining results showed increased mineralized nodule formation in S100A16-siRNA treated BMSCs than in the scramble control (Fig. 2B and C), indicating that S100A16 knockdown promoted osteogenic differentiation of BMSCs and in turn revealing the

inhibitory role of S100A16 in this biological process. In addition, the expression of genes associated with osteogenic differentiation, including RUNX family transcription factor 2 (RUNX2), Osterix (OSX, also known as Sp7 transcription factor), Osteocalcin (OCN, also known as bone gamma-carboxygluta-mate protein), and alkaline phosphatase (ALP), was significantly increased in S100A16-knockdown BMSCs (Fig. 2D), among which the RUNX2 and OSX were also enhanced at the protein level (Fig. 2E). These results confirmed the inhibitory role of S100A16 in the osteogenic differentiation of BMSCs from rats.

Pathways involved in the effects of S100A16 on osteogenic differentiation of rat BMSCs. To elucidate the impact of S100A16 on osteogenic differentiation and identify the underlying biological pathways, transcriptomic sequencing was performed to identify DEGs between scramble control and S100A16-knockdown BMSCs. As demonstrated in Fig. 3A and C, the resulting Venn displayed 358 significantly enriched genes in the S100A16-knockdown groups, with 707 genes downregulated (FDR <0.05, fold change >1.5). Hierarchical clustering of DEGs identified significantly altered gene expression pattern in the si-S100A16 group compared with the control group (Fig. 3B). Furthermore, these DEGs were analyzed through GO function analysis. As shown in Fig. 3D, three ontologies, including biological processes, cellular components and molecular functions of the transcripts due to S100A16 silencing, were identified. In addition, GSEA confirmed a significant upregulation of osteogenic gene set (Fig. 3E) and downregulation of adipogenic genes in the S100A16-silenced transcriptome (Fig. 3F). Notably, it was further recognized that S100A16 knockdown profoundly affected the Smad signaling pathway (Fig. 3G), indicating the potential functional role of Smad in the effect of S100A16 on the osteogenic differentiation of BMSCs.

Roles of Smad4 and MAPK/JNK pathways in the effects of S100A16 on the osteogenic differentiation of rat BMSCs. Previous studies have reported that Smad4 plays a dominant regulatory role in osteogenesis (23-25). Hence, the interactions between S100A16 and Smad4, as well as the involved mitogen-activated protein kinase (MAPK)/c-Jun N-terminal kinase (JNK) signaling pathways were examined. First, Smad4 expression in BMSCs from OVX rats was significantly repressed at both the mRNA (Fig. 4A) and protein levels (Fig. 4B). Meanwhile, the phosphorylation of MAPK and JNK was significantly upregulated (Fig. 4B and C), indicating that the MAPK/JNK pathways were involved in osteogenic differentiation. Subsequently, the effects of S100A16 overexpression on Smad4 and MAPK/JNK pathways were assessed. Accordingly, the significant overexpression of S100A16 in BMSCs (Fig. 4D) significantly downregulated Smad4 (Fig. 4E and F). Furthermore, S100A16 overexpression significantly enhanced the phosphorylation of MAPK and JNK (Fig. 4F and G). Overall, these findings revealed changes in Smad4 and the MAPK/JNK pathways following ovariectomy and S100A16 overexpression, indicating their roles as mediators in the inhibitory effects of S100A16 on the osteogenic differentiation of rat BMSCs.

Suppression of the MAPK/JNK pathways restores osteogenic differentiation of rat BMSCs. To confirm the regulatory roles of the MAPK/JNK pathways in the osteogenic differentiation of BMSCs, the inhibitors U0126 and SP600125 were utilized
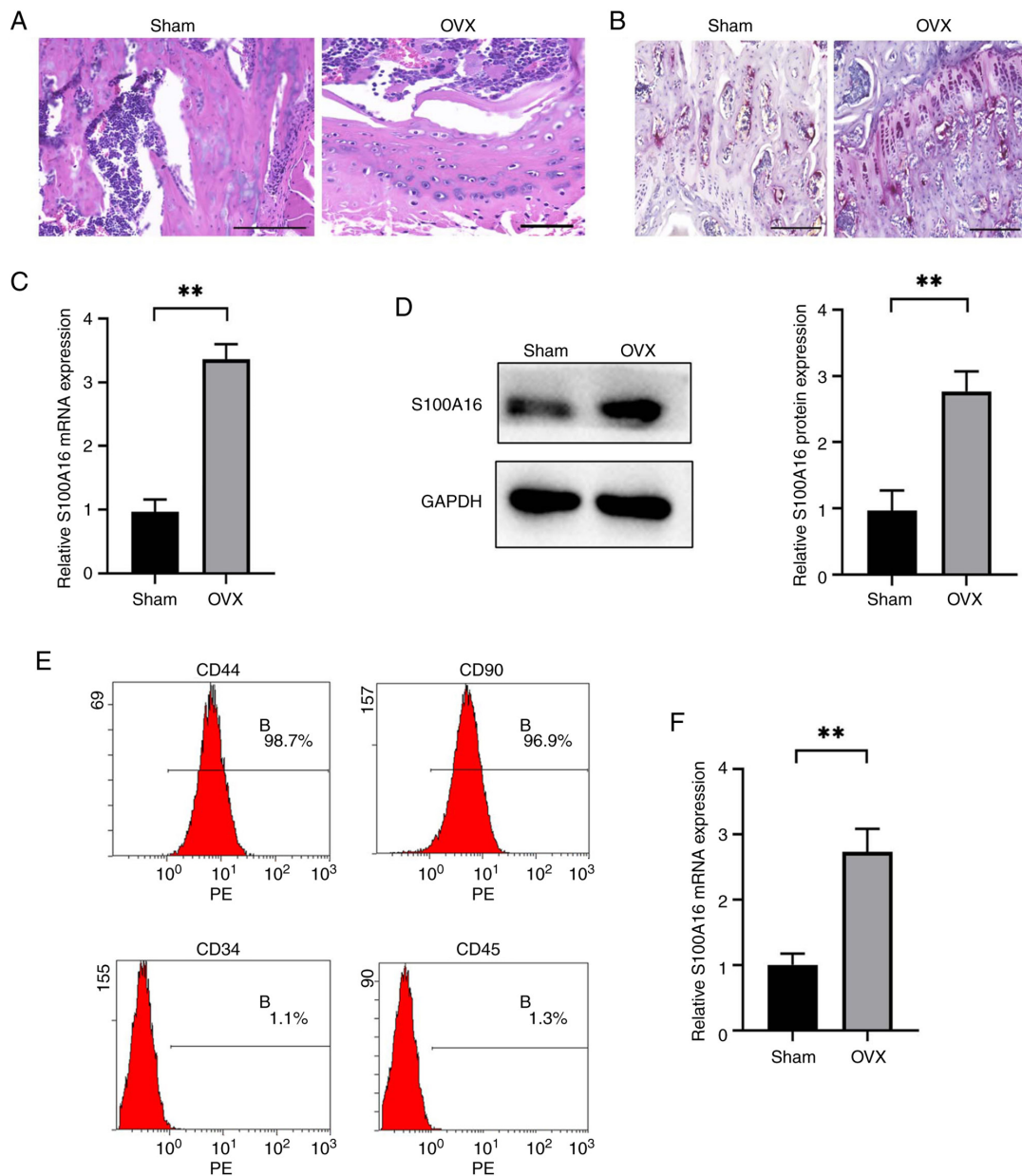
Figure 1. Upregulated S100A16 expression in BMSCs from OVX rats compared with control rats. (A-D) Wild-type rats underwent either sham surgery or bilateral ovariectomy to establish the OVX rat model. (A and B) Representative (A) hematoxylin and eosin staining and (B) Masson's staining of bone tissues from the sham or OVX group to confirm osteoporosis. (C and D) mRNA and protein levels of S100A16 in bone tissues from the sham or OVX group were determined via (C) reverse transcription-quantitative PCR and (D) western blot assays. (E) Representative flow cytometrical plots demonstrating that BMSCs isolated from rat bones were negative for CD34 and CD45 but positive for CD90 and CD44. (F) BMSCs from OVX rats had a higher level of S100A16 expression. [**]P<0.01. BMSCs, bone marrow mesenchymal stem cells; OVX, ovariectomized.

to suppress MAPK and JNK signaling, respectively. The application of these inhibitors efficiently downregulated the phosphorylation of their respective target enzymes in BMSCs isolated from OVX rats without inducing changes in the baseline MAPK/JNK levels (Fig. 5A and B). Furthermore, the effects of MAPK/JNK inhibitors on osteogenic differentiation were compared. As depicted in Fig. 5C, the Alizarin Red S staining results clearly indicated that both inhibitors significantly restored the osteogenic differentiation of BMSCs from OVX rats. Moreover, the effects of MAPK/JNK pathway inhibitors were determined in BMSCs isolated from WT rats with S100A16 overexpression. Similarly, Smad4 levels remained stable, whereas the stimulation of MAPK/JNK phosphorylation

was repressed (Fig. 5D and E). More importantly, both inhibitors alleviated the inhibition of osteogenic differentiation induced by S100A16 overexpression (Fig. 5F). In summary, these results demonstrated that blocking the MAPK/JNK pathways could restore the osteogenic differentiation of BMSCs from both OVX rats and those with S100A16 overexpression, underscoring the inhibitory roles of MAPK/JNK phosphorylation in osteogenic differentiation.

Discussion

The current study investigated the role of S100A16 in the osteogenic differentiation of rat BMSCs and uncovered the underlying
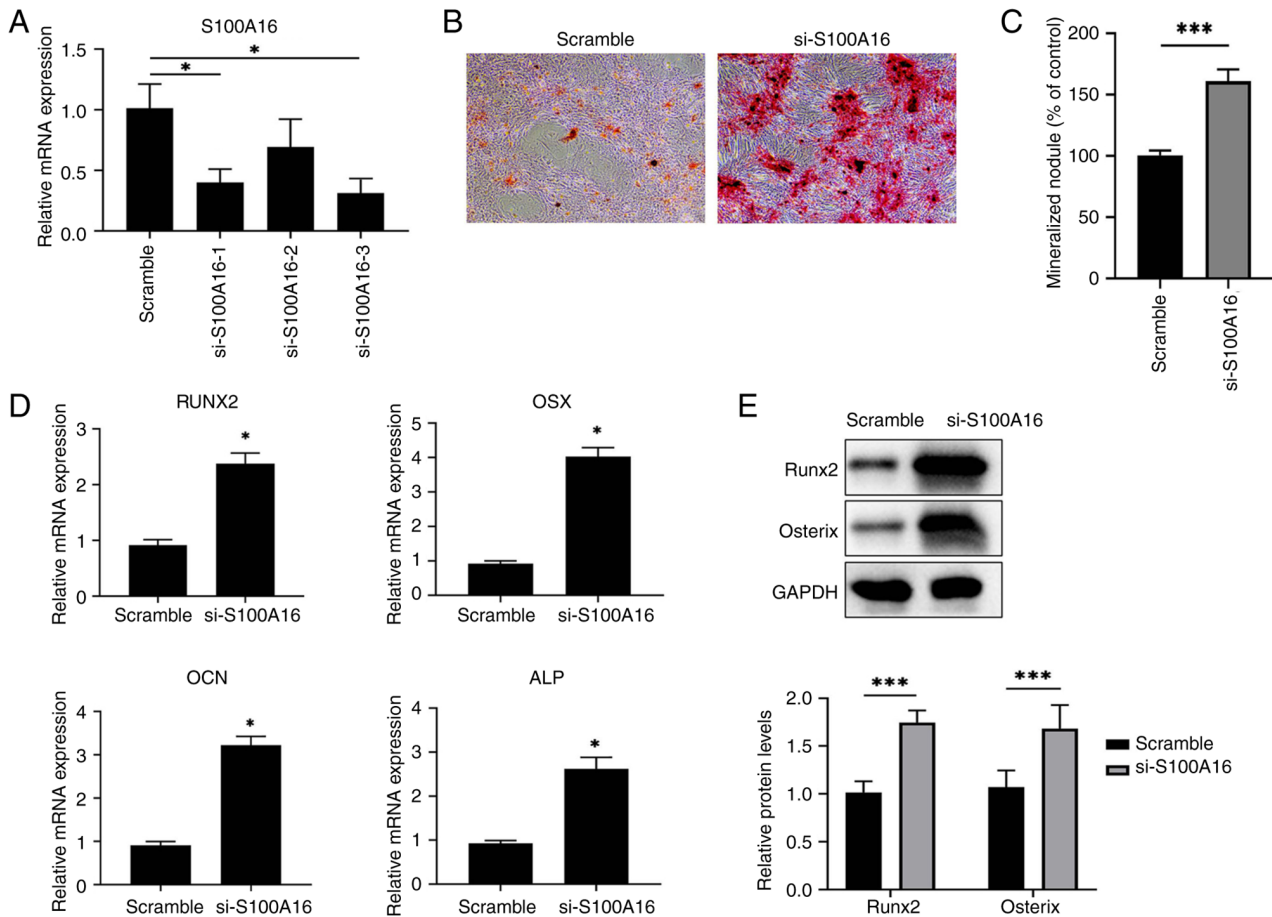
Figure 2. S100A16 silencing promotes osteogenic differentiation of WT BMSCs *in vitro*. (A) Validation of siRNA silencing efficiency in BMSCs isolated from WT rat BMSCs. (B) Representative images for Alizarin Red S staining showed differences in osteogenic differentiation between control rat BMSCs and S100A16-silenced rat BMSCs. (C) Quantification result for Alizarin Red staining. (D) Transfected BMSCs were cultured *in vitro* for 7 days, after which the mRNA expression of Runx2, OSX, OCN and ALP was analyzed via reverse transcription-quantitative PCR. (E) The protein expression of Runx2 and Osterix was analyzed via western blotting. *P<0.05 and ***P<0.001 vs. scramble. BMSCs, bone marrow mesenchymal stem cells; siRNA, small interfering RNA; WT, wild-type; Runx2, RUNX family transcription factor 2; OSX, osterix; OCN, osteocalcin; ALP, alkaline phosphatase.

mechanisms and involved pathways from the perspectives of Smad4 and the MAPK/JNK signaling pathways. Elevated S100A16 levels were first recognized in both bone tissues from OVX rats and isolated BMSCs. S100A16 knockdown promoted osteogenic differentiation, confirming the inhibitory role of S100A16. Furthermore, Smad4 and the MAPK/JNK pathways, identified through transcriptomic sequencing and pathway analysis, were found to be involved in the functional effects of S100A16, as further evidenced by the inhibition of the MAPK/JNK pathways and overexpression of S100A16.

Overall, the current study unveiled the inhibitory role of S100A16 in osteogenic differentiation, as well as the roles of the Smad4 and MAPK/JNK pathways, providing new insights that could help understand osteogenic differentiation. In fact, osteogenic differentiation, the process by which undifferentiated mesenchymal stem cells (MSCs) develop into specialized bone-forming cells called osteoblasts, has been extensively studied. This intricate process involves a series of cellular events regulated by various signaling pathways. Initially, the differentiation of MSCs into osteoblasts is triggered by specific growth factors, such as bone morphogenetic proteins, transforming growth factor-beta (TGF-β) and fibroblast growth factor. These factors activate intracellular signaling cascades, including the

Smad and MAPK pathways, which initiate the expression of key osteogenic genes, including Runx2, OSX and ALP. The present study revealed that changes in S100A16 either via siRNA knockdown or overexpression in rat BMSCs could lead to changes in the MAPK/JNK pathways and in the expression of key genes (Figs. 4 and 5), consequently affecting the osteogenic differentiation. Indeed, other studies using a mouse model (11) or human *in vitro* cell models for osteogenesis (26,27) have confirmed the inhibitory role of S100A16 in this process. As a calcium-binding protein, S100A16 has been implicated in the regulation of various cellular processes, including osteogenic differentiation and bone metabolism (11). The aforementioned findings along with the present results highlight the potential significance of S100A16 as a regulator of osteogenic differentiation and bone homeostasis.

The present study also provided, to the best of the authors' knowledge, the first evidence of the link between S100A16 and Smad4 in osteogenic differentiation, where S100A16 overexpression significantly downregulated the expression of Smad4 (Fig. 4). Smad4 is known as a transcription factor that forms a complex with other Smad proteins upon TGF-β activation. This complex translocases into the nucleus and regulates the expression of targeting genes involved in osteogenic differentiation. In addition, the link between S100A16 and Smad4 has been reported in other
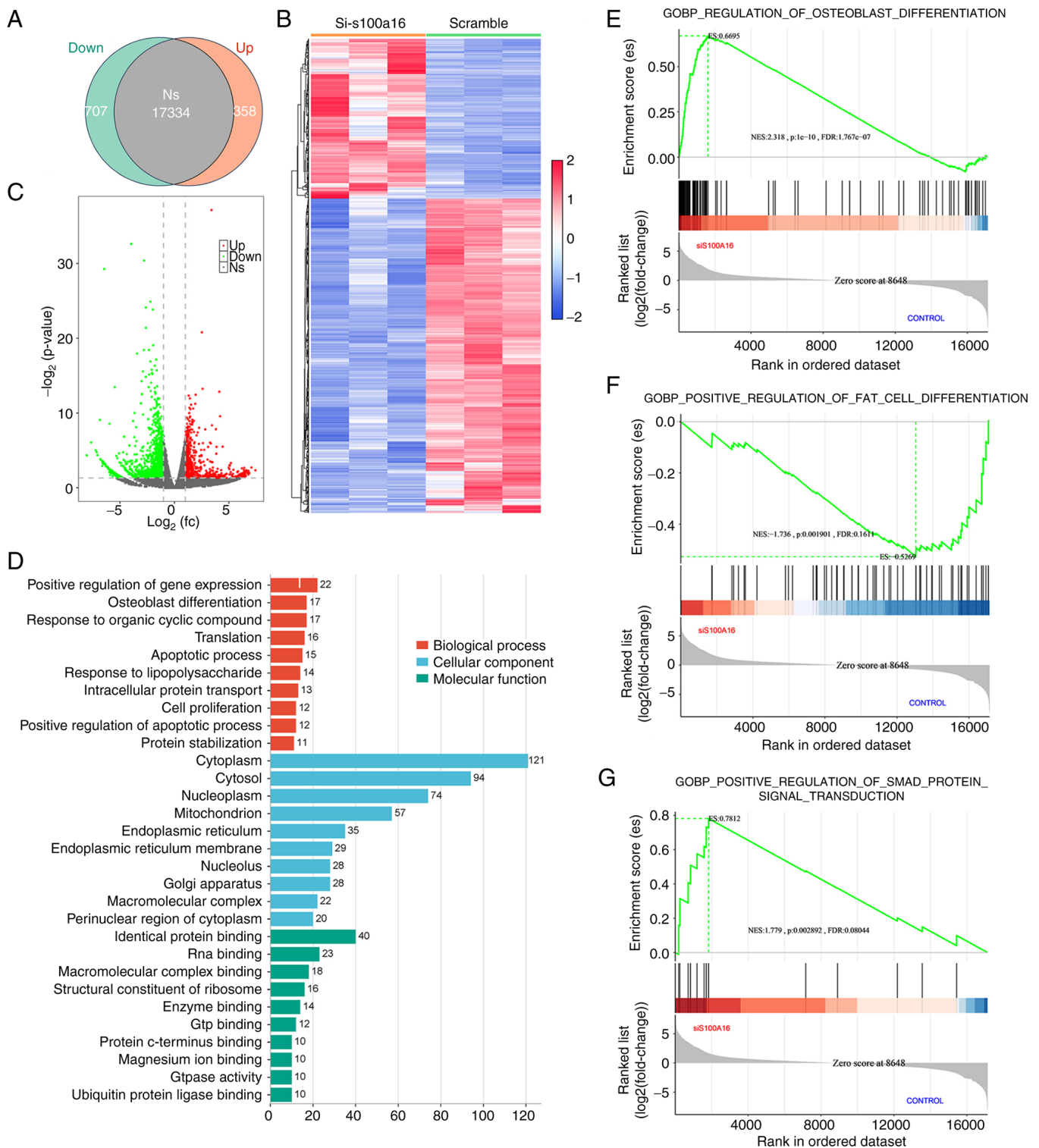
Figure 3. Transcriptome sequencing and bioinformatics analysis identifies that S100A16 silencing significantly impacts the Smad4 signaling pathway. (A) A Venn diagram showing the number of DEGs. A total of 358 and 707 DEGs were upregulated and downregulated, respectively. (B) Hierarchical clustering of DEGs. Columns represent individual experiments, whereas rows correspond to individual genes. Data were normalized and color-coded using the Z-score. (C) Volcano plot demonstrating significant changes in the DEGs between the S100A16-depleted group and control group. Significantly dysregulated genes with P<0.05 are shown as red dots (upregulated) and green dots (downregulated). (D) GO analysis of the upregulated DEGs under S100A16 silencing. Top 10 classification GO function analysis included three ontologies that describe the molecular function, cellular component and biological process of the transcripts, respectively. (E and F) Gene Set Enrichment Analysis revealed that S100A16 depletion was positively associated with (E) osteoblast differentiation and (G) SMAD protein signal transduction gene sets but (F) negatively associated with the fat cell differentiation gene set. DEGs, differentially expressed genes; GO, Gene Ontology.

diseases, especially cancers (28-30). The available knowledge on S100A16 and Smad4 could also provide new insights into the study of the mechanism governing different diseases and potential targets for developing therapeutical strategies.
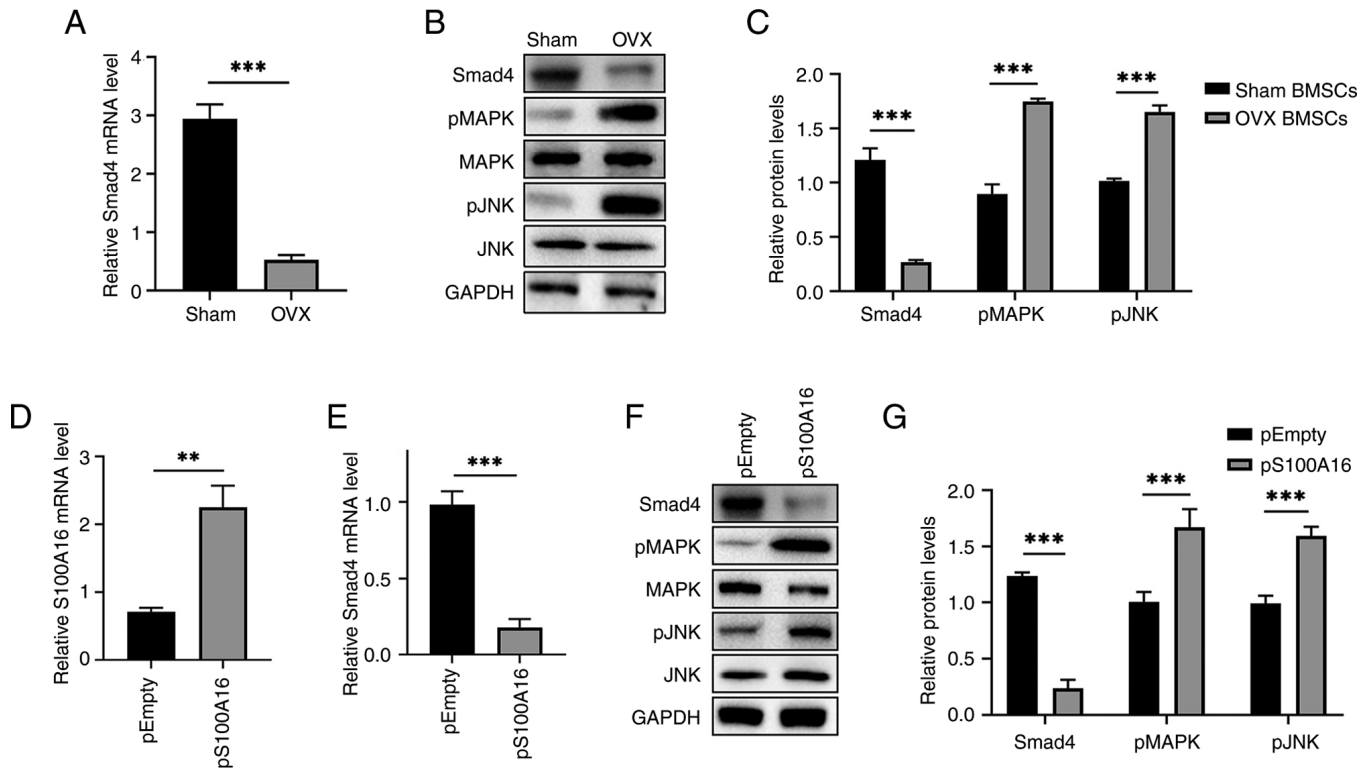
Figure 4. Upregulated S100A16 expression in rat BMSCs downregulates Smad4 expression and activates MAPK/JNK signaling. (A-C) BMSCs from OVX rats exhibited elevated Smad4 expression and increased levels of pMAPK and pJNK. The relative mRNA level of Smad4 in BMSCs from sham and OVX rats was quantified using RT-qPCR. The protein levels of Smad4, pMAPK, and pJNK were assessed via western blot assays. (D and E) BMSCs from WT rats were transfected with either an empty plasmid or an S100A16-expressing plasmid. The mRNA levels of S100A16 and Smad4 were determined via RT-qPCR. (F and G) The relative protein level of Smad4 and the ratios of pMAPK/MAPK and pJNK/JNK in control-transfected and S100A16-expressing plasmid-transfected BMSCs from WT rats were quantified via western blot analysis. $^{**}P<0.01$ and $^{***}P<0.001$. BMSCs, bone marrow mesenchymal stem cells; OVX, ovariectomized; p-, phosphorylated; RT-qPCR, reverse transcription-quantitative PCR; WT, wild-type.

Furthermore, Smad4 had been reported to downregulate JNK activity in human pancreatic carcinoma (31). JNK is a member of the MAPK family. SMAD4 also inhibits thyroid cancer cell growth by inactivating the MAPK/JNK pathway (16). However, the role of MAPK/JNK signaling in osteogenesis appears to be controversial. On the one hand, bone morphogenetic protein-9 had been reported to enhance the osteogenic differentiation of human periodontal ligament stem cells via the JNK pathway (17). On the other hand, another study indicated that the MAPK/JNK signaling pathway suppresses the osteogenic differentiation of MC3T3-E1 osteoblasts exposed to titanium ion (18). In the present study, the inhibition of the MAPK/JNK pathways restored the osteogenic differentiation of BMSCs (Fig. 5). Together, these results revealed that the specific role of the MAPK/JNK pathway in osteogenesis would be context-dependent, with factors including, but not limited to, species, cell type source and exogenous stimulation.

The current study has several potential limitations. First, most of it remained at the level of the *in vitro* cell models, including the BMSCs isolated from WT and OVX rats. Hence, the gap between *in vitro* and *in vivo* models and limitations in the conclusions of the present study that could be extrapolated to *in vivo* models must be acknowledged. Next, the interaction between Smad4 and the MAPK/JNK pathways remains to be explored. Although stable levels of Smad4 were found after MAPK/JNK pathway inhibition, direct evidence is still required for studying the potential interaction between these

two pathways. Finally, other pathways involved in the function of S100A16 in osteogenic differentiation remain to be determined. Together, future studies addressing these limitations are needed to further understand the role of S100A16, as well as other inhibitory factors, in osteogenesis, which would be crucial for developing strategies that promote and enhance osteogenic differentiation for potential therapeutic applications in bone tissue engineering and regenerative medicine.

In summary, the role of S100A16 in the osteogenic differentiation of rat BMSCs was investigated. The current study uncovered a novel mechanistic link between S100A16 and Smad4, as well as the MAPK/JNK signaling pathways, in osteogenic differentiation. Further studies on these key impact factors may ultimately contribute to the development of preventive and therapeutic strategies for osteoporosis.

Acknowledgements
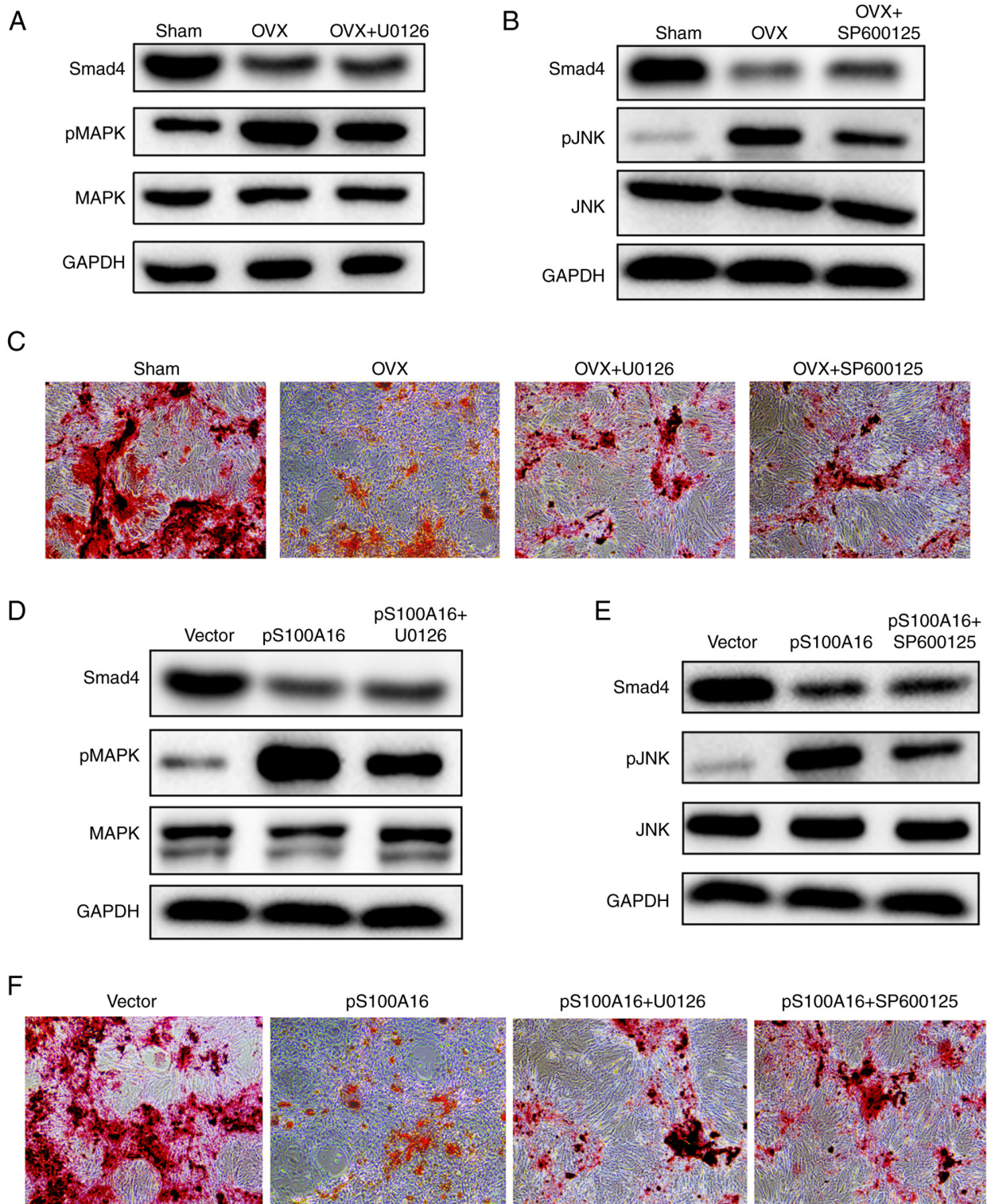
Figure 5. Inhibition of the MAPK/JNK pathway restores the osteogenic differentiation of BMSCs from OVX rats or S100A16-overexpressing wild-type rat BMSCs. (A) Western blot assay confirmed the effective downregulation of MAPK signaling in BMSCs isolated from OVX rats upon treatment with the MAPK inhibitor U0126. (B) Western blot assay confirmed the successful downregulation of JNK signaling in BMSCs isolated from OVX rats after treatment with the JNK inhibitor SP600125. (C) A comparison of Alizarin Red S staining results among the indicated groups. (D) Western blot assay confirmed the downregulation of MAPK signaling in S100A16-overexpressed BMSCs upon treatment with the MAPK inhibitor U0126. (E) Western blot assay confirmed the downregulation of JNK signaling in S100A16-overexpressed BMSCs after treatment with the JNK inhibitor SP600125. (F) Alizarin Red S staining of BMSCs transfected with either control empty plasmid or S100A16-overexpressing plasmid with or without treatment with MAPK inhibitor U0126 or JNK inhibitor SP600125. BMSCs, bone marrow mesenchymal stem cells; OVX, ovariectomized; p-, phosphorylated.

Availability of data and materials

The data generated in the present study may be found in the Gene Expression Omnibus under accession number GSE259238 or at the following URL: https://www.ncbi.nlm.nih.gov/geo/query/acc.cgi?acc=GSE259238.

Authors' contributions

JX and YafS conceived the study, designed the experiments and interpreted the results. JX, YanS, JB and ZW performed the experiments, and collected and analyzed the data. JX and JB confirm the authenticity of all the raw data. JX wrote the manuscript. JB and YafS revised the manuscript. YafS supervised the study. All authors read and approved the final manuscript.

Ethics approval and consent to participate

The animal study protocol was approved (approval no. 2020018) by Luohe Central Hospital Animal Ethics Committee (Luohe, China).

Patient consent for publication

Not applicable.

Competing interests

The authors declare that they have no competing interests.

References

1. Fedarko NS: Osteoblast/osteoclast development and function in osteogenesis imperfecta. Osteogenesis Imperfecta. Academic Press, pp45-56, 2014.
2. Kim JM, Lin C, Stavre Z, Greenblatt MB and Shim JH: Osteoblast-osteoclast communication and bone homeostasis. Cells 9: 2073, 2020.
3. Zhang J, Zhang X, Zhang L, Zhou F, van Dinther M and Ten Dijke P: LRP8 mediates Wnt/β-catenin signaling and controls osteoblast differentiation. J Bone Miner Res 27: 2065-2074, 2012.
4. Day TF, Guo X, Garrett-Beal L and Yang Y: Wnt/beta-catenin signaling in mesenchymal progenitors controls osteoblast and chondrocyte differentiation during vertebrate skeletogenesis. Dev Cell 8: 739-750, 2005.
5. Yamaguchi A, Komori T and Suda T: Regulation of osteoblast differentiation mediated by bone morphogenetic proteins, hedgehogs, and Cbfa1. Endocr Rev 21: 393-411, 2000.
6. Skillington J, Choy L and Derynck R: Bone morphogenetic protein and retinoic acid signaling cooperate to induce osteoblast differentiation of preadipocytes. J Cell Biol 159: 135-146, 2002.
7. Gaur T, Lengner CJ, Hovhannisyan H, Bhat RA, Bodine PV, Komm BS, Javed A, van Wijnen AJ, Stein JL, Stein GS and Lian JB: Canonical WNT signaling promotes osteogenesis by directly stimulating Runx2 gene expression. J Biol Chem 280: 33132-33140, 2005.
8. Yang W, Li HY, Wu YF, Mi RJ, Liu WZ, Shen X, Lu YX, Jiang YH, Ma MJ and Shen HY: ac4C acetylation of RUNX2 catalyzed by NAT10 spurs osteogenesis of BMSCs and prevents ovariectomy-induced bone loss. Mol Ther Nucleic Acids 26: 135-147, 2021.
9. Zhang B, Zhang X, Xiao J, Zhou X, Chen Y and Gao C: Neuropeptide Y upregulates Runx2 and osterix and enhances osteogenesis in mouse MC3T3-E1 cells via an autocrine mechanism. Mol Med Rep 22: 4376-4382, 2020.
10. Lee KM, Park KH, Hwang JS, Lee M, Yoon DS, Ryu HA, Jung HS, Park KW, Kim J, Park SW, *et al*: Inhibition of STAT5A promotes osteogenesis by DLX5 regulation. Cell Death Dis 9: 1136, 2018.
11. Li D, Zhang R, Zhu W, Xue Y, Zhang Y, Huang Q, Liu M and Liu Y: S100A16 inhibits osteogenesis but stimulates adipogenesis. Mol Biol Rep 40: 3465-3473, 2013.
12. Sturchler E, Cox JA, Durussel I, Weibel M and Heizmann CW: S100A16, a novel calcium-binding protein of the EF-hand superfamily. J Biol Chem 281: 38905-38917, 2006.
13. Liu DD, Zhang JC, Zhang Q, Wang SX and Yang MS: TGF-β/BMP signaling pathway is involved in cerium-promoted osteogenic differentiation of mesenchymal stem cells. J Cell Biochem 114: 1105-1114, 2013.
14. Zhang LT, Liu RM, Luo Y, Zhao YJ, Chen DX, Yu CY and Xiao JH: Hyaluronic acid promotes osteogenic differentiation of human amniotic mesenchymal stem cells via the TGF-β/Smad signalling pathway. Life Sci 232: 116669, 2019.
15. Zhao M, Mishra L and Deng CX: The role of TGF-β/SMAD4 signaling in cancer. Int J Biol Sci 14: 111-123, 2018.
16. Cai H, Yang X, Jiang Z, Liang B, Cai Q and Huang H: Upregulation of SMAD4 inhibits thyroid cancer cell growth via MAPK/JNK pathway repression. Trop J Pharm Res 18: 2473-2478, 2019.
17. Wang P, Wang Y, Tang W, Wang X, Pang Y, Yang S, Wei Y, Gao H, Wang D and Cao Z: Bone morphogenetic protein-9 enhances osteogenic differentiation of human periodontal ligament stem cells via the JNK pathway. PLoS One 12: e0169123, 2017.
18. Zhu WQ, Ming PP, Zhang SM and Qiu J: Role of MAPK/JNK signaling pathway on the regulation of biological behaviors of MC3T3-E1 osteoblasts under titanium ion exposure. Mol Med Rep 22: 4792-4800, 2020.
19. Lei Z, Xiaoying Z and Xingguo L: Ovariectomy-associated changes in bone mineral density and bone marrow haematopoiesis in rats. Int J Exp Pathol 90: 512-519, 2009.
20. Du D, Zhou Z, Zhu L, Hu X, Lu J, Shi C, Chen F and Chen A: TNF-α suppresses osteogenic differentiation of MSCs by accelerating P2Y$_2$ receptor in estrogen-deficiency induced osteoporosis. Bone 117: 161-170, 2018.
21. Chen W, Chen X, Chen AC, Shi Q, Pan G, Pei M, Yang H, Liu T and He F: Melatonin restores the osteoporosis-impaired osteogenic potential of bone marrow mesenchymal stem cells by preserving SIRT1-mediated intracellular antioxidant properties. Free Radic Biol Med 146: 92-106, 2020.
22. Livak KJ and Schmittgen TD: Analysis of relative gene expression data using real-time quantitative PCR and the 2(-Delta Delta C(T)) method. Methods 25: 402-408, 2001.
23. Song B, Estrada KD and Lyons KM: Smad signaling in skeletal development and regeneration. Cytokine Growth Factor Rev 20: 379-388, 2009.
24. Park JS, Kim M, Song NJ, Kim JH, Seo D, Lee JH, Jung SM, Lee JY, Lee J, Lee YS, *et al*: A reciprocal role of the Smad4-Taz axis in osteogenesis and adipogenesis of mesenchymal stem cells. Stem Cells 37: 368-381, 2019.
25. Pakravan K, Razmara E, Mahmud Hussen B, Sattarikia F, Sadeghizadeh M and Babashah S: SMAD4 contributes to chondrocyte and osteocyte development. J Cell Mol Med 26: 1-15, 2022.
26. Gu H, Huang Z, Yin X, Zhang J, Gong L, Chen J, Rong K, Xu J, Lu L and Cui L: Role of c-Jun N-terminal kinase in the osteogenic and adipogenic differentiation of human adipose-derived mesenchymal stem cells. Exp Cell Res 339: 112-121, 2015.
27. Li Y, Wagner ER, Yan Z, Wang Z, Luther G, Jiang W, Ye J, Wei Q, Wang J, Zhao L, *et al*: The calcium-binding protein S100A6 accelerates human osteosarcoma growth by promoting cell proliferation and inhibiting osteogenic differentiation. Cell Physiol Biochem 37: 2375-2392, 2015.
28. Su Y, Qi R, Li L, Wang X, Li S, Zhao X, Hou R, Ma W, Liu D, Zheng J and Shi M: An immune-related gene prognostic risk index for pancreatic adenocarcinoma. Front Immunol 13: 945878, 2022.
29. Wang R, Wu Y, Yu J, Yang G, Yi H and Xu B: Plasma messenger RNAs identified through bioinformatics analysis are novel, non-invasive prostate cancer biomarkers. Onco Targets Ther 13: 541-548, 2020.
30. Leclerc E and Vetter SW: The role of S100 proteins and their receptor RAGE in pancreatic cancer. Biochim Biophys Acta 1852: 2706-2711, 2015.
31. Zhang X, Cao J, Pei Y, Zhang J and Wang Q: Smad4 inhibits cell migration via suppression of JNK activity in human pancreatic carcinoma PANC-1 cells. *Oncol Lett* 11: 3465-3470, 2016.